**THE EUROPEAN
PHYSICAL JOURNAL E**

Regular Article - Flowing Matter

Structural aspects of an energy-based water classification index and the structure–dynamics link in glassy relaxation

Alejandro R. Verde[1], Joan Manuel Montes de Oca[1,2], Sebastián R. Accordino[1], Laureano M. Alarcón[1], and Gustavo A. Appignanesi[1,a]

[1] Departamento de Química, INQUISUR, Universidad Nacional del Sur (UNS)-CONICET, Avenida Alem 1253, 8000 Bahía Blanca, Argentina
[2] Pritzker School of Molecular Engineering, University of Chicago, Chicago, IL 60637, USA

Abstract An energy-based structural indicator for water, V_4, has been recently introduced by our group. In turn, in this work we aim at: (1) demonstrating that V_4 is indeed able to correctly classify water molecules between locally structured tetrahedral (T) and locally distorted (D) ones, circumventing the usual problem of certain previous indicators of overestimating the distorted state; (2) correlating V_4 with dynamic propensity, a measure of the molecular mobility tendency, in order to seek for the existence of a connection between structure and dynamics within the supercooled regime. More specifically, in the first part of this work we will show that V_4 accurately discriminates between merely thermally deformed local molecular arrangements and truly distorted molecules (defects). This fact will be made evident not only from radial distribution function results but also from the dynamic propensity distributions of the different kinds of molecules. In turn, we shall devote the second part of this work to finding correlations between T and D molecules with low- and high-dynamic-propensity molecules, respectively, thus revealing the existence of a link between local structure and dynamics, while also making evident the dominant role of the D molecules (defects) in the structural relaxation. Moreover, the availability of a proper molecular classification technique will enable us to study the timescale of such influence of structure on dynamics by defining a modified dynamic propensity measure and by applying it to the structured and unstructured water molecular states.

1 Introduction

When we cool a liquid below its melting point fast enough to avoid crystallization, the relaxation quickly slows down as the system enters the so-called supercooled regime [1–15]. If we continue cooling down, the relaxation behavior gets progressively more sub-diffusive until, eventually, the system falls out of equilibrium and we are left with a glass [1–15]. But astonishingly, this dramatic dynamical slowing down, or glassy dynamics, is accompanied by almost no noticeable structural change [1–15]. In fact, the determination of the existence a clear causal link between structure and dynamics has remained quite elusive despite certain interesting recent advances by computer simulations and, particularly, by the introduction of the concept of dynamic propensity (the tendency of the molecules to significantly move away from their position at a given initial configuration) [16–27]. Dynamic propensity represents a powerful indirect measure that indeed signals the existence of regions of the sample with different structural constraints but tells us noth-

ing on the nature of such local constraints. It is thus relevant to try to find correlations between dynamic propensity and direct structural indicators, a fact that is complicated for glassforming systems where the local molecular environments are not easy to classify.

Being water a structured liquid, it becomes natural to explore the possible existence of such a structure-dynamics connection for its supercooled state. Besides, water represents a system of great intrinsic interest where the emergence of a sub-diffusive behavior (not only below but also above the melting point in certain contexts like nanoconfinement or interfaces) becomes central for many scientific and technological fields [1,24,28–51]. Indeed, the dynamic propensity approach has been preliminary applied to supercooled water with partial success [24–27]. However, to ultimately unravel the existence of a causal link between structure and dynamics for water, the employment of an appropriate structural indicator to correlate with dynamic propensity is still demanded. Several structural indices have been indeed introduced in the past [24,33–37,37,52–62]. Such indicators have been built on the basis of particular structural aspects of the local molecular order present in water (like the degree of tetrahedrality of the

[a] e-mail: appignan@criba.edu.ar (corresponding author)

first coordination shell or the degree of translational order up to the second shell). Thus, these approaches have been able to detect molecules with well-developed local order and molecules belonging to a locally distorted or unstructured state. However, in our group we have recently built an energy-based new index, called V_4 [63], that avoids introducing any structural preconception. Moreover, our results suggested that the population of the distorted state might have been mostly overestimated by certain previous indicators, since certain molecules with a local first shell that is deformed by thermal fluctuations are, instead, found to belong to well-structured configurations if such masking effect is properly subtracted [63]. Under this scenario, the present work is thus devoted to investigate structural details of the V_4-classification and, more importantly, to study the correlations between V_4 and the dynamic propensity measure in order to elucidate the existence of clear connections between structure and dynamics in supercooled water.

2 Methods

2.1 Water model and simulation details

We conducted molecular dynamics (MD) simulations of the SPC/E [64] water model by using the GROMACS package version 5.0.2 [65]. Bonds were constrained with the LINCS algorithm and long-range electrostatics evaluated with the PME method. The time step used was 2 fs. A modified Berendsen thermostat and a Parrinello–Rahman barostat at 1 bar as reference pressure were used. We built cubic boxes of appropriate sizes with periodic boundary conditions and a cutoff of 1nm for the short-range forces. The SPC/E system consisted of 1050 water molecules. This size is appropriate for the dynamic propensity approach where a large number of different realization within the isoconfigurational ensemble are demanded (we used 100 isoconfigurational runs for $T = 210$ K and 1000 runs for $T = 240$ K; in both cases we also averaged over many different replicas to gain statistics). After equilibration for times much larger than the structural relaxation (the α relaxation time) for each temperature, production data runs were produced. We also employed the inherent structures scheme to suppress the masking effect of thermal vibrations that difficult structural classification at the real trajectory. This approach [66] partitions the potential energy surface (PES) of the system into disjoint basins, the set of configuration space points that belong to the same local minimum (inherent structure, IS) when subject to a minimization process. Thus, from any given instantaneous structure of the MD trajectory (at the real dynamics) we applied a steepest-descent algorithm until convergence (largest scalar force on any atom being lower than 10 kJ/mol nm within a maximum number of steps of 100,000).

2.2 The $V_4(i)$ structural indicator for water

The V_4 index [63] involves the calculation of all pairwise interactions V_{ij}, $j \neq i$ for each water molecule i and ordering them in intensity, from the lowest to the largest value. Then, $V_4(i)$ is defined as the forth V_{ij}. A molecule with a well-structured, tetrahedrally arranged first coordination shell will present a $V_4(i)$ value close to that for a linear hydrogen bond (HB) energy, while a molecule with a distortion in its tetrahedral arrangement will yield a higher $V_4(i)$ value. This index presents clear bimodal distributions both at the real and the inherent dynamics [63], being the latter scheme the correct one for structural classification purposes [63]. This fact enables us to classify water molecules as locally structured or unstructured beyond the estimation of the fraction of the two states, a possibility that is out of reach for most of the older indicators [63]. Later on, we shall additionally provide further arguments to show that the energetically based V_4 index also corrects the tendency to overestimate the fraction of unstructured molecules in which certain structurally based indicators tend to incur [63].

2.3 The dynamic propensity measure

The isoconfigurational ensemble (IC) [16] is defined as a set of equal length molecular dynamics trajectories or runs (on the order of the α relaxation time) starting from the same initial configuration (same molecular positions) but with momenta randomly chosen from a Boltzmann distribution corresponding to the system's temperature. Within the glassy relaxation regime, each IC run presents dynamical heterogeneities (certain regions of the system move much faster than others) but mobility is not reproducible: the more mobile molecules differ from one run of the IC to another one [16]. The dynamic propensity of the molecules for a time interval of length t is calculated as [16]: $DP = < \Delta \mathbf{r}_i^2 >_{IC}$ (where $< ... >_{IC}$ involves averaging over all the runs of the IC and $\Delta \mathbf{r}_i^2 = (\mathbf{r}_i(t = t) - \mathbf{r}_i(t = 0))^2$ represents the squared displacement of molecule i for the interval starting from the initial configuration and ending at time t). However, during this work we shall also calculate propensity values by averaging over different subintervals within this timescale. At low temperatures, that is, within the supercooled regime, this process produces an heterogeneous distribution of dynamic propensities with the highest propensity molecules tending to spatially arrange in rather compact clusters within the sample [16–23]. This result points to the fact that the initial structure indeed determines the dynamical tendency of the molecules to move away from the starting configuration [16–23]. Such influence of structure on dynamics for times commensurate with the α relaxation time comes from the confinement of the system within the local metabasin of the potential energy surface, PES, (a metabasin is a set of mutually similar structures separated from other metabasins by large barriers) until a collective movement, called a d-cluster,
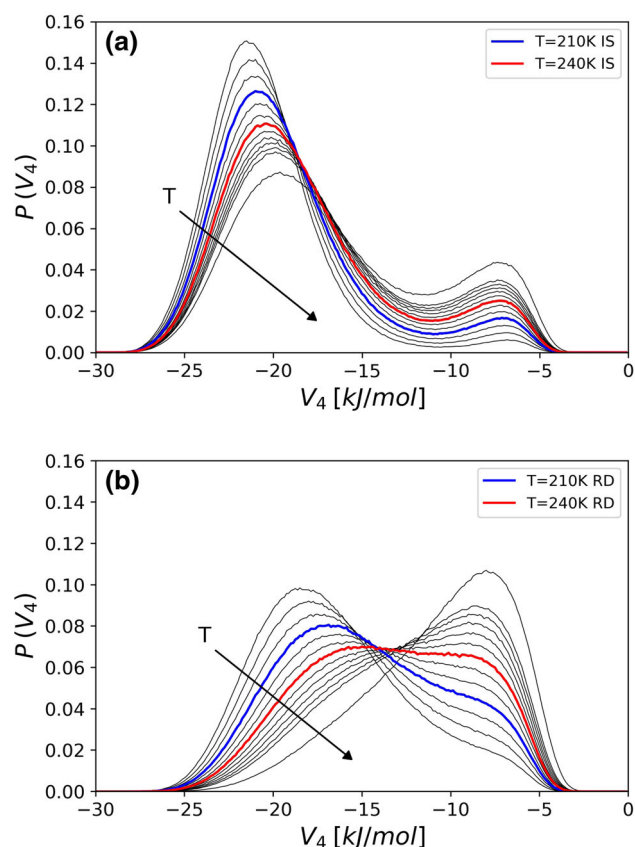
Fig. 1 Distributions of the V_4 index calculated both at **a** the inherent dynamics (inherent structures, IS) and **b** real dynamics (RD), for SPC/E water and a series of temperatures (from temperatures above the melting point to temperatures within the supercooled regime; arrows indicate the direction of increasing temperature)

allows it to abandon the current metabasin [19,20]. In this work, we use 1000 IC runs for $T = 240\,\mathrm{K}$ and 100 for $T = 210\,\mathrm{K}$, also averaging over many independent replicas for each temperature. The length of the runs is on the order of the α relaxation time for each temperature, a timescale when most of the IC runs have been able to abandon the local metabasin [14,19,20]. Specifically, the α relaxation time, or τ_α, is estimated as the time when the intermediate incoherent scattering function, measured at the wave vector of the first peak in the structure factor, has decayed to $1/e$ and is around 769 ps at $T = 210$ K and 35ps at $T = 240$ K; basically, at this timescale the molecules have moved on average one intermolecular distance and the system has been able to leave the plateau of the mean squared displacement plot consistent with the caging regime.

3 Results and discussion

3.1 Molecular classification and structural details

Figure 1 displays the distributions of the indicator V_4 for a series of temperatures and pressure of 1 bar, both at the real and inherent dynamics. While neat bimodality behavior is evident in both schemes, the inherent dynamics approach is the one that allows for a correct classification of molecular classes, as already shown [63]. This fact holds not only from structural considerations, as similarity of the radial distribution functions to experimental results on high and low density amorphous water, but also from the capability of allowing a proper description of the anomalous behavior of water's heat capacity [63]. The peak on the left of the inherent dynamics V_4 distribution (lower or more negative values) comprises molecules with four well-tetrahedrally arranged high-quality linear HBs (such molecules are thus called as T molecules), while the peak on the right is populated by molecules where the tetrahedral arrangement is distorted and (at least) one HB has been loosen (the D molecules). Thus, the peak on the left corresponds to structured molecules while the peak on the right represents unstructured ones. For classification purposes, we consider a threshold value that lies in between the two peaks of the V_4 distribution, $V_4 = -12\,\mathrm{kcal/mol}$, but moderate changes in this value do not alter significantly our results. We note that we have observed the existence of fivefold coordinated molecules [63], but differently from the case of the 3-fold coordinated ones, these penta-coordinated molecules are always very few and their fraction does not change much with temperature. Additionally, these molecules present a V_4 value characteristic of the tetrahedral ones (good tetrahedral coordination with four high-quality HBs) while still able to form a rather good fifth interaction. Thus, the small number of fivefold coordinated molecules will be included within the T ones. D molecules, in turn, comprise threefold coordinated molecules since they imply basically the neat rupture of a HB and their fraction changes significantly with temperature.

While from now on we shall classify water molecules as T or D with V_4 at the inherent dynamics, it is nonetheless relevant to note that at the real dynamics distribution of V_4 there are many molecules from the right peak ($V_4 > -12\,\mathrm{kcal/mol}$) that would move to the left peak ($V_4 < -12\,\mathrm{kcal/mol}$) upon minimization (when we change to the inherent dynamics scheme). These T molecules (as the classification at the inherent dynamics indicates), however, would look much like a D molecule at the real dynamics. In fact, they present thermally deformed arrangements at the real dynamics, but the minimization process shows that they indeed belong to a well-structured basin (T-basin). For practical purposes, while indeed belonging to the T-state in our classification, we shall also term them as F molecules (since they could be thought as false D molecules: They appear as D at the real dynamics but when the thermal disorder is removed they become T ones). Structural indicators based merely on structural preconceptions (at difference from the V_4 index that is based on energy considerations) would misclassify most of these molecules as unstructured. For exam-
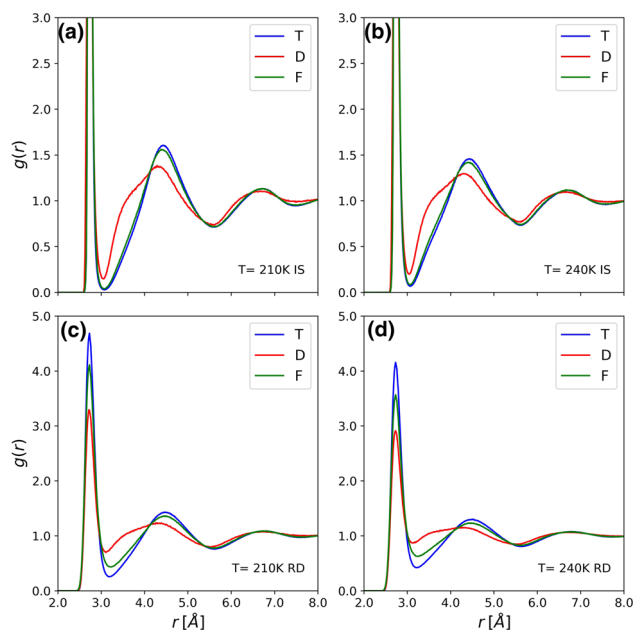
Fig. 2 Radial distribution functions for the T, D and F molecules at the real dynamics (RD) and inherent dynamics (inherent structures, IS) for SPC/E water for $T = 210$ K and $T = 240$ K

ple, the local structure index (LSI, an index that is based on the translational order of the first and the second coordination shells [24,34–37,37,52,53,60]) clearly overestimates the population of the unstructured state (we note that we will always refer to the LSI evaluated at the inherent structures level where, at variance form the case at the real dynamics, it is able to yield neat bimidal distributions). Indeed, this state is the dominant one for LSI, even well within the supercooled regime [24,34–37,37,60], which is at odds from the results we show in Fig. 1 where the T molecules are the predominant ones. Such concern on the overestimation of unstructured molecules by certain merely structure-based indicators is quite relevant if we intend to find a link between structure and dynamics. We note that there also exist other structural parameters like the local order metric which measures the degree of order as compared to a suitable reference system [67,68]. It would be interesting to compare the results of this indicator at the inherent dynamics scheme with V_4 in future work.

It is known that structured molecules tend to present a clear gap between the first and the second coordination shell (that allows the first shell to develop a proper tetrahedral coordination) and that, in turn, unstructured molecules imply certain collapse of the second shell, with one or more molecules occupying interstitial positions and hence perturbing the local order of the first shell (Fig. 2). However, a recent work suggests that the unstructured molecules might be less disordered than expected and that they indeed show certain structural preferences [69]. To make this whole picture more precise, we now present the radial distribution

functions, RDFs, for the T and D molecules and also for the F molecules (that we now consider as a subset of the T molecules and which, as already indicated, might be regarded as unstructured on the basis of their thermally deformed local environments). Figure 2 displays such RDFs both at the real and minimized (IS) configurations.

If we compare the RDFs of the T and D molecules (at both schemes, real and inherent dynamics), we find clear differences between them. While T molecules display a pronounced gap between the first and second peaks (corresponding to the first and second coordination shells, respectively), the D molecules exhibit an important population in such region, a clear indication of the presence of interstitial molecules. However, not all interstitial positions are equally probable but there is a notable peak (or shoulder). In turn, the RDFs of the F molecules at the real dynamics do in fact present certain population in the inter-peak region but evidently no peak or shoulder is noticeable. Indeed, the RDFs at the IS scheme show that the interstitial peak is even more evident for the D molecules upon minimization, while the inter-peak region is clearly depopulated for the F molecules, making the curves almost identical to that of the T molecules at such minimized scheme. These results undoubtedly point to the fact that, if we intend to search for connections between structure and dynamics within the supercooled regime, it is mandatory to discriminate between merely thermally deformed molecules and truly distorted ones (that is, defects). Thus, in the following we shall use the V_4 index at the IS scheme to classify water molecules and in order to search for correlations with dynamic propensity.

3.2 Correlations between local structure and dynamic propensity measures

As already indicated, the dynamic propensity measure determines the tendency of the water molecules to move away from their positions at any given initial configuration. In turn, we have also learnt that the V_4 indicator provides us with the ability to properly classify the local structure of the water molecules. Thus, in this section we will seek for correlations between both quantities in order to elucidate the existence of a clear link between structure and dynamics for water in the glassy regime. Thus, starting from a given initial configuration we classify the molecules as T, D and F at such initial configuration (time $t = 0$) and calculate their dynamic propensity distributions for the time interval that goes from $t = 0$ to the time of the structural or α relaxation time, $t = \tau_\alpha$. (We recall that F molecules are in fact a subset of the T molecules; they are well-structured molecules that would be misclassified as unstructured on the basis of merely structural considerations).

Figure 3 shows the results. It is evident that the propensity distribution of the T molecules is centered at lower values as compared to that for the D molecules. Thus, the well-structured molecules indeed display, on average, a markedly lower mobility tendency than the
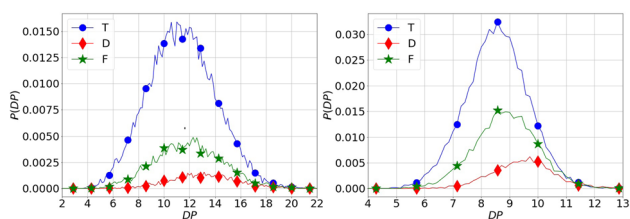
Fig. 3 Propensity distribution for the time interval ($t = 0, t = \tau_\alpha$) for the T, D and F molecules (SPC/E water for $T = 210\,\mathrm{K}$, left, and $T = 240\,\mathrm{K}$, right). We measure dynamic propensity in units of $\mathring{A}^2$. The curves are not normalized in order to evidence the relative abundances. The sum of the three curves gives the full normalized propensity distribution
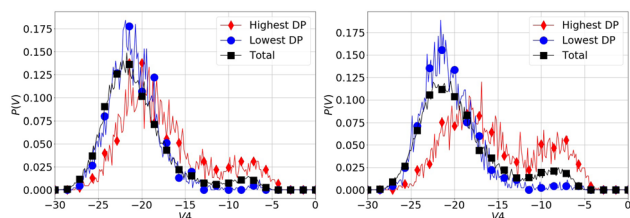

Fig. 4 V_4 distribution for the molecules with the 10% highest and 10% lowest propensity for SPC/E water for $T = 210\,\mathrm{K}$ (left) and $T = 240\,\mathrm{K}$ (right). The distributions for all the water molecules are also included for comparison

unstructured ones. In turn, we note that the propensity distribution for the F molecules is very similar to the one for the T ones, again confirming the fact that the F molecules are just thermally excited T molecules. This reinforces the relevance of not overestimating the unstructured state by including merely thermally deformed molecules. If a portion of the T-state would be misclassified, as the existence of the F molecules reveals, the signs of the correlation between structure and dynamics would be spoiled or even completely blurred. Thus, from now on, we shall just focus on T and D molecules, that is, molecules classified with the V4 distribution at the inherent dynamics.

In turn, in Fig. 4 we show the V_4 distributions (at the IS level) for the molecules with highest and lowest dynamic propensity values. Since the propensity distribution is not bimodal, at variance form the V_4 distribution, we choose as high-propensity molecules the ones that present the 10% highest values, while we term as low-propensity molecules the ones that are within the 10% lowest values. From Fig. 4, it is evident that the low-propensity molecules are almost all well-structured (the distribution virtually includes no D molecules), while the high-propensity ones significantly enrich their population in D molecules as compared to the global V_4 distribution, that is, the one for all the water molecules. This, in accord with the results of Fig. 3, also speaks of the existence of a correlation between local structure and dynamics, a link that emerges clearly only when the water molecules are classified in a correct manner.

In general, the population of F molecules (molecules that would be classified as D in the real dynamics, RD, but that become T after minimizing, that is, at the Inherent Structures, IS) is significant. That is, many molecules change identity when applying the V_4 index at the RD or IS . However, we expect that the change in identity for the molecules within the 10% highest (or 10% lowest) propensity set would be less frequent. At $T = 210\,\mathrm{K}$, we have that globally 6% of the water molecules are D and 94% are T molecules (at the IS). For the 10% highest propensity set of molecules, we are interested mainly in the D molecules (more mobile should correlate with unstructured). For this subset, we have that 17% of them are D at the IS (this makes sense since the defects are scarce, see also Fig. 4). And all of them are also D when we use the V_4 index at the RD, that is, they conserve identity by passing form IS to RD. We also find that 94% of them are also classified as unstructured by the LSI index at the IS (low LSI values; for the LSI calculation procedure, please see [34, 35]). In turn, for the subset of molecules within the 10% lowest propensity, we are interested in the structured molecules (T, that should be less mobile). Interestingly, 99% of this subset is T at the IS (in agreement with Fig. 4) and 88% of them still keep being T at the RD. However, only 58% of them are classified as structured by the LSI index at the IS (molecules with high LSI), a fact that again speaks of the overestimation this index makes of the unstructured state.

To further illustrate the link between local structure and dynamics, in Fig. 5 we correlate V_4 with the dynamic propensity measure for $T = 210\,\mathrm{K}$ and T=240K. The contour plots present the full data (they also contain the more restricted information which we have used in Figs. 3 and 4) and thus provide us with further interesting insights. First of all, it is evident that the regions of the T (large spot in Fig. 5) and D (small spot in Fig. 5) molecules are centered at different dynamical propensity values, with the D ones located at the right (higher dynamic propensity values). In turn, there are no significant correlations between V_4 values and dynamic propensity within each of the two regions of Fig. 5. Thus, the behavior is found to be rather digital: While the degree of structural order or potential energy within a molecular class does not present a significant influence on dynamic propensity, an evident increase is indeed expected, on average, when changing from the T to the D class, that is, upon becoming a defect. Another interesting observation is that the molecules within the 10% lowest propensity set (values below the first vertical line) are exclusively T molecules. That is, this region made up of very slow or highly constrained molecules contains only low-V_4 well-structured molecules which form four good HBs and, thus, have low local energy as compared to the D ones. A previous interesting work [25] had sought for correlations between potential energy and dynamic propensity in supercooled water. But given the poor results with the instantaneous potential energy, an isoconfigurational-ensemble averaged potential energy, that is, a potential energy propensity (a measure that does not rely
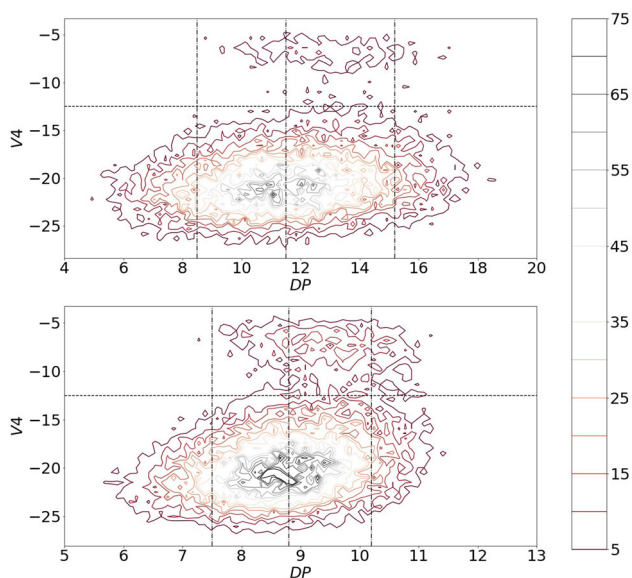
Fig. 5 Contour plots of the correlation of V_4 and dynamic propensity for SPC/E water for $T = 210$ K (top) and $T = 240$ K (bottom). In each case, the horizontal line indicates the threshold to classify molecules as T and D, while the vertical lines indicate the values that define the 10% lowest propensity molecules, the mean propensity and the 10% highest propensity molecules. In both cases, the large spot at lowest V_4 values (the region with the highest population) is that of the structured, T molecules, while the small spot contains the unstructured, or D ones

only on the initial structure but that is averaged over a certain number of configurations during the relaxation dynamics of the different IC runs) had to be employed to characterize the potential energy of the molecules. In such work, a correlation between low potential energy molecules and low dynamic propensity was found (in accord with our results), while no correlation could be found at the other side of the energy spectrum (high-potential-energy molecules did not correlate with high dynamic propensity) [25]. However, Fig. 5 shows that the D molecules (small spot in the contour plot) indeed reside in the region of high dynamic propensity: above the mean propensity value also enriching their contribution to the region of the 10% highest propensity molecules. This correlation between structural defects and molecular mobility in water's relaxation dynamics is now evident thanks to the fact that we are furnished with a structural indicator with an accurate classification capability, the V_4 index. Moreover, we recall that we have had no need to resort to an isoconfigurational-ensemble averaged quantity (that is, a propensity-based quantity that explicitly includes dynamical information in its definition) in order to quantify the local molecular structure or the molecular potential energy. Instead, V_4 is a direct structural measure which is indeed calculated solely at the initial structural configuration.

In turn, in Fig. 6 and to better illustrate the results, we provide three-dimensional plots for a typical configuration at T = 201K. We show the same view of the box
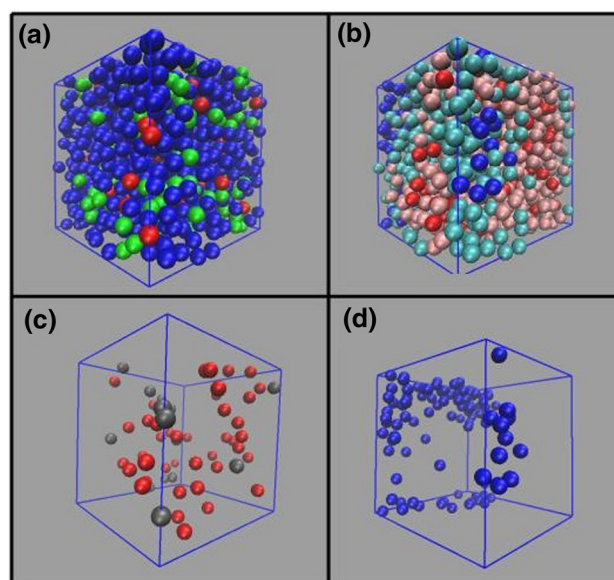

Fig. 6 Three-dimensional plot of the same typical configuration at $T = 210$ K (we show the same view of the simulation box in all cases; for simplicity, water molecules are represented by spheres). **a** 3D plot with molecules classified according to their molecular kind: D in red, F in green and T in blue; **b** propensity classes: All the molecules with dynamic propensity higher than the mean value are shown in red color (the ones with the 10% highest values colored in dark red and the rest in light red), while the molecules with propensity values lower than the mean are shown in blue (dark blue for the ones with the 10% lower values and light blue otherwise); **c** D molecules, colored in red if they have a propensity value higher than the mean or gray otherwise; **d** molecules within the 10 percent lowest propensity values colored in blue if they are T or F molecules while depicted in gray otherwise (in this case none of them is D so there are no molecules in gray color)

but illustrating four instances: Fig. 6a shows the different molecular kinds for all the molecules in the box; Fig. 6b shows the different propensity classes; Fig. 6c depicts the D molecules classified by their propensity; and Fig. 6d shows the molecules within the 10% lowest propensity values classified according to their structural class defined by V_4. Direct inspection of Fig. 6 b) shows certain clustering tendency for the molecules with high and low propensity, while Fig. 6c shows that D molecules are clearly enriched in high propensity values, and Fig. 6d shows the great dominance of structured molecules for the ones with the 10% lowest propensity (in this case none of them is D). All this is consistent with the results shown in our previous figures.

Finally, while the former results imply that the local structure does indeed exert an influence on the subsequent dynamics of the water molecules, it is also interesting to determine the timescale of such influence. In other words, we now wish to study how long the memory of the initial structure persists on molecular mobility. It is well established that the glassy relax-
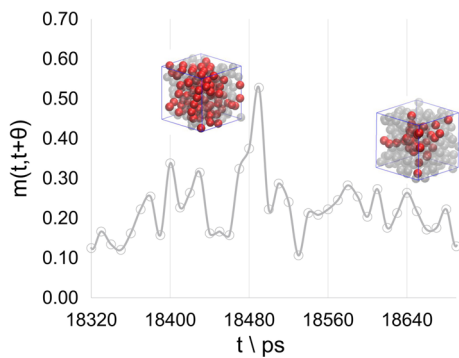
Fig. 7 Function $m(t, t+\theta)$ with $\theta = 10ps$ for a portion of a typical run at $T = 210$ K, showing the fraction of molecules that have moved more than $1\mathring{A}$ in each time interval. We also include the three-dimensional plot for the time when a d-cluster occurs ($t = 18,490$ ps) and for a time when the system displays a typical relaxation behavior (in each case we indicate in red the water molecules that have moved more than $1\mathring{A}$ in the corresponding 10ps time window)

ation regime for a supercooled liquid is governed by the presence of dynamical heterogeneities: The existence of regions of the sample that relax faster than the others, a phenomenon that is maximum at a timescale that lies within the α relaxation time [4,6,8–10,14]. Within this scenario, our group has shown in the past that the local relaxation proceeds by means of fast collective movements of particles arranged in relatively compact clusters, called d-clusters, that drive the system from one local metabasin of its potential energy landscape to a neighboring one [10–14,19,20]. In Fig. 7, we show an example of a typical d-cluster for a portion of one of the water trajectories at T=210 K. We show the function $m(t, t+\theta)$, for $\theta = 10ps$ (the fraction of molecules that have moved more than $1\mathring{A}$ in consecutive time intervals of 10 ps, a timescale close to 1% of the α relaxation time at this temperature). While most of the time this function presents low values (the system does not exhibit significant mobility), the existence of a clear peak is evident at t=18490 ps indicating that the system is undergoing a significant mobility event, a d-cluster. We also include the three-dimensional plot of this d-cluster event (depicting the mobile molecules, that is, the ones that moved more than $1\mathring{A}$ in 10 ps) and an example of a typical time window when no d-cluster occurs (few molecules moved more than $1\mathring{A}$ in 10 ps).

Additionally, we have shown for a model glass former (binary Lennard–Jones mixture) that the occurrence of a d-cluster decorrelates the dynamic propensity map, that is, the initially high-propensity molecules cease to be so upon the occurrence of a d-cluster event and are then replaced by a new set of high-propensity particles [19,21–23]. The description that emerges is that the initially high-propensity particles are less retained at their original positions within the initial configuration and thus display an enhanced tendency to move away from them in all the different IC runs. These isolated unconcerted movements are not successful for some time until

these molecules are able to perform a coherent collective movement, a d-cluster. However, each IC run develops a somewhat different d-cluster, each run at a different time within the α relaxation time. The d-cluster, in turn, makes the system to abandon the local metabasin where it had been confined so far, so that the particles are finally able to relax their local environments. Thus, the particles which exhibited a high dynamic propensity value at the initial configuration are then replaced by a new set of high-propensity particles for the trajectory under consideration. However, this structural decorrelation process has not been amenable of a direct study in model glass formers like the binary Lennard-Jones mixture, since the way to define a well-structured or an unstructured local environment for the particles is not obvious for such systems. Provided the accurate structural classification capability of the V_4 index, water represents a proper system where to tackle this problem by determining the duration of the high-propensity character of unstructured molecules. To this end, we classify water molecules as T and D exclusively at a given initial configuration (that is, $t = 0$, the common origin of the different IC trajectories), and we now compute propensity measures on different time intervals. Specifically, we divide the whole time interval $[t = 0, t = \tau_\alpha]$ into ten equally spaced time intervals and we calculate:
$DP_t(i,j) = <\Delta\mathbf{r}_i^2(j)>_{IC}$, where $\Delta\mathbf{r}_i^2(j) = (\mathbf{r}_i(t = (j/10)\tau_\alpha) - \mathbf{r}_i(t = ((j-1)/10)\tau_\alpha))^2$, with $j = 1, 2, ...10$.

In other words, we calculate dynamic propensity values for the ten time intervals, each one of equal duration $(1/10)\tau_\alpha$: In each case, we measure the squared displacements of the particles during the corresponding time interval, and we average over all the trajectories of the IC. However, we recall that, while propensity is calculated within different time intervals, all the IC runs start, as always, at $t = 0$, the same starting configuration where molecules are classified as D or T. We then proceed to average the propensity values (we average over all the i molecules) in order to get the function $ADP_t(j)$.

Figure 8 shows $ADP_t(j)$ as a function of j, by discriminating the behavior for T and D molecules (we average over T and D molecules separately). As the index j increments, it means that the calculation of the dynamic propensity is performed over a (always equal duration) time interval that is progressively shifted toward τ_α. We show the results at $T = 210$ K since the propensity distribution is broader (more heterogeneous) as temperature decreases, but similar results are obtained for $T = 240$ K. In accord with the results of Fig. 3, the curves show that the dynamic propensity values for the D molecules at the first time intervals are higher than that for the T molecules. However, as time increases (as we calculate propensity for time intervals whose beginning moves toward τ_α), the average dynamic propensity of the D molecules decreases toward that of the T molecules and the difference practically vanishes before τ_α. The T molecules, in turn, display a practically constant value, making evident the fact that they are not relevant in terms of the structural relaxation events. On the contrary, the decreasing value
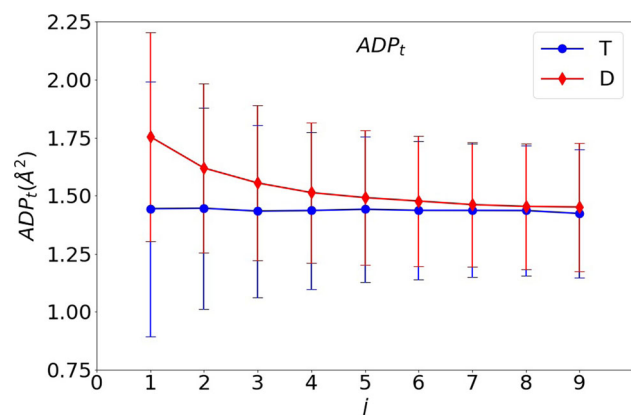
Fig. 8 The function $ADP_t(j)$ calculated for the T and D molecules (classified at the initial configuration) for SPC/E water and $T = 210$ K as a function of time (an increase in the value of the index j corresponds to a time interval located at a later time, that is, the time interval of length $\tau_\alpha/10$, is shifted in $(j-1)\tau_\alpha/10$). Error bars are indicated in the graph

of ADP_t with j for the D molecules implies that these molecules are indeed the main actors in terms of the structural relaxation, that is, they are the molecules that mainly take part in d-cluster events. Each IC trajectory presents a d-cluster event at a different time involving a subset of all the initial D molecules. Once the d-cluster has occurred, the structural constraints of the initial configuration are modified and, thus, the high-propensity molecules cease to present an enhanced mobility for the corresponding IC trajectory at such time. As time increases toward τ_α, more and more IC runs have produced a d-cluster and, thus, the value of ADP_t for the D molecules continues falling toward that of the T molecules.

4 Conclusions

In the present work, we employed the V_4 water structural indicator (a new energy-based index recently introduced by our group) and correlated it with the dynamic propensity of the water molecules (their tendency to be mobile) within the supercooled regime. First, we showed that a merely geometrically based structural classification (as most previous structural indicators, like the local structure index or LSI, employ) may overestimate the population of the distorted state. To this end, we classified molecules as tetrahedral (T) and distorted (D) ones, but also identified a subclass within the T ones, namely the F molecules. The F molecules look much like D ones on geometrical terms, but we showed them to represent merely thermally deformed structures that nonetheless belong to a T energy basin (when the thermal noise is removed by means of an energy minimization). Thus, F molecules should not be confused with truly distorted molecules or defects, the D ones. This fact was made evident form

the analysis of the radial distribution functions of F molecules, which showed a great similarity to the ones for the T molecules and a clear difference form that of the D ones. We also showed that the F molecules display a dynamic propensity distribution very similar to that of the T ones, revealing that they are less prone to mobility than the D molecules and further revealing that they are indeed a subset of the T molecules. A recent work provided very interesting evidences pointing to the crucial role of the network connection (and percolation) of molecules of the same class [70]. Thus, it would be interesting to pursue a similar analysis with this new classification scheme. However, we must note that D molecules tend to be a small fraction of the system (more at low temperatures) and, while they show certain clustering tendency [63], are mostly surrounded by T molecules. Thus, while T and D molecules indicate two different molecular arrangements, the LDA-like state is expected to be virtually purely composed of T molecules, while the HDA-like state consists of a mixture of T and D molecules [63] (LDA refers to low density amorphous ice and HDA to high density amorphous ice). Hence, a proper two-state picture of water might not be simply based on single-molecule properties but, instead, on two different local multi-molecule environments: one almost purely tetrahedral (only T) and one distorted (T and D) [63]. We plan to perform further work in this direction.

In turn, we showed that the T molecules exhibit a dynamic propensity distribution peaked at a lower value than that of the D molecules, thus making evident the existence of a firm link between structure and dynamics for the glassy regime of water. We also analyzed the V_4 distributions of the sets of molecules with highest and lowest propensity values to confirm that they are clearly enriched in D and T molecules, respectively. Finally, being furnished for the first time with an accurate molecular classification tool (V_4) we were able to define a new dynamic propensity measure in order to study the timescale of the influence of the local structure on the dynamics. In doing so, we found that the initial variance of structural constraints decreases in time to fade out within the structural or α relaxation time. This enabled the following molecular picture of the mutual interplay between structure and dynamics in water's glassy relaxation: Any given configuration is characterized by the presence of initially high-propensity molecules. This set of molecules contains both T (structured) and D (unstructured) molecules, but is clearly enriched in D as compared to the global composition. In turn, the set of lowest propensity molecules (which are rather immobile for the timescale under consideration) contains only T molecules (virtually no defects, D). The high-propensity molecules are uncomfortable at their initial positions and, thus, try to move away from them in the different runs of the isoconfigurational ensemble, IC. However, these individual movements do not succeed to locally relax the system until a coherent concerted motion of the different molecules occur, the so-called d-cluster. Upon such expedient, the system is then able to aban-

don the local metabasin of the potential energy landscape where it had been confined so far and the initial local structural constraints are thus recast. Since the d-clusters for the distinct IC runs occur at different times within the α relaxation time, it is only at such timescale that the memory from the initial structure is completely lost, as can be learnt form the decay of the dynamic propensity of the defective D molecules at time intervals close to τ_α. Then, a different set of molecules is subject to looser local structural constraints that affect their ulterior dynamical behavior, thus becoming the new high-propensity molecules.

To summarize, in this work we showed that molecular motion in supercooled water is indeed conditioned by the local structure, with defects (distorted, D molecules) playing a dominant role in the relaxation dynamics. In turn, we revealed that the duration of such influence of structure on dynamics is local in time, fading out at a timescale commensurate with the α relaxation time.

Author contribution statement

All authors have contributed equally to this work.

References

1. P.G. Debenedetti, *Metastable Liquids* (Princeton University Press, Priceton, NJ, 1996)
2. C.A. Angell, Science **267**, 1924 (1995). https://doi.org/10.1126/science.267.5206.1924
3. W. Kob, C. Donati, S.J. Plimpton, P.H. Poole, S.C. Glotzer, Phys. Rev. Lett **79**, 2827 (1997). https://doi.org/10.1103/physrevlett.79.2827
4. C. Donati, J.F. Douglas, W. Kob, S.J. Plimpton, P.H. Poole, S.C. Glotzer, Phys. Rev. Lett. **80**, 2338 (1998). https://doi.org/10.1103/physrevlett.80.2338
5. C. Donati, S.C. Glotzer, P.H. Poole, Phys. Rev. Lett. **82**, 5064 (1999a). https://doi.org/10.1103/physrevlett.82.5064
6. M.D. Ediger, Ann. Rev. Phys. Chem. **51**, 99 (2000). https://doi.org/10.1146/annurev.physchem.51.1.99
7. C.A. Angell, K.L. Ngai, G.B. McKenna, P.F. McMillan, S.W. Martin, J. App. Phys. **88**, 3113 (2000). https://doi.org/10.1063/1.1286035
8. E.R. Weeks, J.C. Crocker, A.C. Levitt, A. Schofield, D.A. Weitz, Science **287**, 627 (2000). https://doi.org/10.1126/science.287.5453.627
9. S.C. Glotzer, Physics of Non-Crystalline Solids 9. J. Non-Cryst. Solids **274**, 342 (2000). https://doi.org/10.1016/s0022-3093(00)00225-8
10. G.A. Appignanesi, J.A. Rodriguez Fris, R.A. Montani, W. Kob, Phys. Rev. Lett. **96**, 057801 (2006). https://doi.org/10.1103/physrevlett.96.057801
11. G.A. Appignanesi, J.A. Rodriguez Fris, J. Phys.: Condens. Matter **21**, 203103 (2009). https://doi.org/10.1088/0953-8984/21/20/203103
12. J.A. Rodriguez Fris, G.A. Appignanesi, E.R. Weeks, Phys. Rev. Lett. **107**, 065704 (2011)
13. J.A. Rodriguez Fris, E.R. Weeks, F. Sciortino, G.A. Appignanesi, Phys. Rev. E **97**, 060601(R) (2018)
14. J.A. Rodriguez Fris, G.A. Appignanesi, E. La Nave, F. Sciortino, Phys. Rev. E **75**, 041501 (2007)
15. J.M. Montes de Oca, S.R. Accordino, G.A. Appignanesi, P.H. Handle, F. Sciortino, J. Chem. Phys. **150**, 144505 (2019)
16. A. Widmer-Cooper, P. Harrowell, H. Fynewever, Phys. Rev. Lett. **93**, 135701 (2004)
17. A. Widmer-Cooper, P. Harrowell, Phys. Rev. Lett. **96**, 185701 (2006)
18. A. Widmer-Cooper, P. Harrowell, J. Chem. Phys. **126**, 154503 (2007)
19. G.A. Appignanesi, J.A. Rodriguez Fris, M.A. Frechero, Phys. Rev. Lett. **96**, 237803 (2006)
20. J.A. Rodriguez Fris, L.M. Alarcón, G.A. Appignanes, Phys. Rev. E **76**, 011502 (2007)
21. M.A. Frechero, L.M. Alarcón, E.P. Schulz, G.A. Appignanesi, Phys. Rev. E **75**, 011502 (2007)
22. J.A. Rodriguez Firs, L.M. Alarcón, G.A. Appignanesi, J. Chem. Phys. **130**, 024108 (2009)
23. D. Malaspina, E.P. Schulz, M.A. Frechero, G.A. Appignanesi, Phys. A **388**, 3325 (2009)
24. D.C. Malaspina, J.A. Rodriguez Fris, G.A. Appignanesi, F. Sciortino, EuroPhys. Lett. **88**, 16003 (2009)
25. G.S. Matharoo, M.S. Gulam Razul, P.H. Poole, Phys. Rev. E **74**, 050502(R) (2006)
26. M. Fitzner, G.C. Sosso, S.J. Cox, A. Michaelides, Proc. Natl. Acad. Sci USA **116**, 2009 (2019)
27. A.R. Verde, J.M. Montes de Oca, S.R. Accordino, L.M. Alarcón, Gustavo A. Appignanesi, J. Chem. Phys. **150**, 244504 (2019)
28. P.H. Poole, F. Sciortino, U. Essmann, H.E. Stanley, Nature **360**, 324 (1992)
29. P.G. Debenedetti, H.E. Stanley, Phys. Today **56**, 40 (2003)
30. O. Mishima, H.E. Stanley, Nature **396**, 329 (1998)
31. C.A. Angell, Chem. Rev. **102**, 2627 (2002)
32. C.A. Angell, Ann. Rev. Phys. Chem. **55**, 559 (2004)
33. J. Russo, H. Tanaka, Nat. Commun. **5**, 3556 (2014)
34. G.A. Appignanesi, J.A. Rodriguez Fris, F. Sciortino, Eur. Phys. J. E **29**, 305 (2009)
35. S.R. Accordino, J.A. Rodriguez Fris, F. Sciortino, G.A. Appignanesi, Eur. Phys. J. E **34**, 48 (2011)
36. S.R. Accordino, D.C. Malaspina, J.A. Rodriguez Fris, G.A. Appignanesi, Phys. Rev. Lett. **106**, 029801 (2011)
37. J.M. Montes de Oca, J.A. Rodriguez Fris, S.R. Accordino, D.C. Malaspina, G.A. Appignanesi, Eur. Phys. J. E **39**, 124 (2016)
38. P. Ball, Proc. Natl. Acad. Sci. U.S.A. **114**, 13327 (2017)
39. D.M. Huang, D. Chandler, Proc. Natl. Acad. Sci. U.S.A. **97**, 8324 (2000)
40. X. Huang, C.J. Margulis, B.J. Berne, Proc. Natl. Acad. Sci. U.S.A. **100**, 11953 (2003)

41. N. Giovambattista, P.G. Debenedetti, C.F. Lopez, P.J. Rossky, Proc. Natl. Acad. Sci. U.S.A. **105**, 2274 (2008)
42. A. Bizzarri, S. Cannistraro, J. Phys. Chem. B **106**, 6617 (2002)
43. D. Vitkup, D. Ringe, G.A. Petsko, M. Karplus, Nat. Struct. Biol. **7**, 34 (2000)
44. N. Choudhury, B. Montgomery Pettitt, J. Phys. Chem. B **109**, 6422 (2005)
45. H.E. Stanley, P. Kumar, L. Xu, Z. Yan, M.G. Mazza, S.V. Buldyrev, S.-H. Chen, F. Mallamace, Physica A **386**, 729 (2007)
46. E.P. Schulz, L.M. Alarcón, G.A. Appignanesi, Eur. Phys. J. E **34**, 114 (2011)
47. D.C. Malaspina, E.P. Schulz, L.M. Alarcón, M.A. Frechero, G.A. Appignanesi, Eur. Phys. J. E **32**, 35 (2010)
48. L.M. Alarcón, D.C. Malaspina, E.P. Schulz, M.A. Frechero, G.A. Appignanesi, Chem. Phys. **388**, 47 (2011)
49. S.R. Accordino, D.C. Malaspina, J.A. Rodriguez Fris, L.M. Alarcón, G.A. Appignanesi, Phys. Rev. E **85**, 031503 (2012)
50. S.R. Accordino, J.M. Montes de Oca, J.A. Rodriguez Fris, G.A. Appignanesi, J. Chem. Phys. **143**, 154704 (2015)
51. J.M. Montes de Oca, C.A. Menéndez, S.R. Accordino, D.C. Malaspina, G.A. Appignanesi, Eur. Phys. J. E **40**, 78 (2017)
52. E. Shiratani, M. Sasai, J. Chem. Phys. **104**, 7671 (1996)
53. E. Shiratani, M. Sasai, J. Chem. Phys. **108**, 3264 (1998)
54. P.-L. Chau, A.J. Hardwick, Mol. Phys. **93**, 511 (1998)
55. J.R. Errington, P.G. Debenedetti, Nature **409**, 318 (2001)
56. I. Naberukhin Yu, V.P. Voloshin, N.N. Medvedev, Mol. Phys. **73**, 917 (1991)
57. A. Oleinikova, I. Brovchenko, J. Phys. Condens. Matter **18**, S2247 (2006)
58. M.J. Cuthbertson, P.H. Poole, Phys. Rev. Lett. **106**, 115706 (2011)
59. R. Shi, H. Tanaka, J. Chem. Phys. **148**, 124503 (2018)
60. J. Gelman Constantin, A. Rodriguez Fris, G. Appignanesi, M. Carignano, I. Szleifer, H. Corti, Eur. Phys. J. E **34**, 126 (2011)
61. K.T. Wikfeldt, A. Nilsson, L.G.M. Pettersson, Phys. Chem. Chem. Phys. **13**, 19918 (2011)
62. B. Santraa, R.A. DiStasio Jr., F. Martelli, R. Car, Mol. Phys. **113**, 2829 (2015)
63. J.M. MontesdeOca, F. Sciortino, G.A. Appignanesi, J. Chem. Phys. **152**, 244503 (2020)
64. H.J.C. Berendsen, J.R. Grigera, T.P. Straatsma, J. Phys. Chem. **91**, 6269 (1987)
65. H.J.C. Berendsen, D. van der Spoel, R. van Drunen, Comput. Phys. Commun. **91**, 43 (1995)
66. F.H. Stillinger, *Energy Landscapes, Inherent Structures, and Condensed-Matter Phenomena* (Princeton University Press, Princeton, 2015)
67. F. Martelli, H.-Y. Ko, E.C. Oğuz, Phys. Rev. B **97**, 064105 (2018)
68. F. Martelli, H.-Y. Ko, C. Calero Borallo, G. Franzese, Front. Phys. **13**, 136801 (2018)
69. J.M. Montes de Oca, S.R. Accordino, A.R. Verde, L.M. Alarcón, G.A. Appignanesi, Phys. Rev. E **99**, 062601 (2019)
70. F. Martelli, J. Chem. Phys. **150**, 094506 (2019)